

## EXPERIMENTAL DESIGN

### Reactor-Analysis System

Figures 1 and 2 display the reactor-analysis system. Provisions are made to monitor one to three thermocouples, a pressure transducer, and the IR active light gases evolved during a devolatilization experiment. The temperature, total pressure and light gas data generated are real time data.

Power to the grid is provided by a programmable power supply (Harrison Model 6269A) operated in one of two modes. In the voltage programmed mode, the voltage delivered to the grid in any instant is determined by a voltage and time selection system (VATS), which will be described in detail elsewhere. Up to five step function increments, both plus and minus, in the grid voltage can be made. The duration of the increments are independently selectable. The response time of the power supply is 20 msec or less.

In the current program mode the screen is forced to conduct a constant current. The voltage across the screen floats to maintain the constant current condition. In the current and time select (CATS) mode, the heating rate and final temperature of the screen are coupled as previously noted (1,2). Figures 3 and 4 display typical temperature vs time plots obtained with each control system.

For synchronization, the FTIR is the master and all other electronic circuits (VATS, CATS, high speed camera, solenoid valve, etc.) are slaves.

Attempts to monitor the real time temperature of the grid by placing small (~75-100  $\mu\text{m}$  dia) thermocouple beads between the folds of the grid produced inconsistent results particularly for heating rates of  $\geq 10^3$  C/sec and final temperatures  $\geq 800$  C. Voltages were frequently induced across the thermocouple bead/leads as were indicated by discontinuities in the temperature-time curves. In the worst case, measured potentials (thermal plus induced) exceeded the maximum allowable for chromel-alumel thermocouples.

Consequently, the temperature of the grid system was monitored by spot welding the beads to the underside of the bottom fold of the grid. Even in this case, care had to be taken to insure a single-spot weld, as it was observed that welds with two or more contact points again produced spurious voltages across the bead. One to three thermocouples attached at different points to the grid could be monitored. Although sampling rates of 2 kHz are possible with the data acquisition system, thermocouple sampling rates of 500 Hz were commonly used. Figures 3 and 4 show typical temperature versus time plots for blank screen runs with the VATS and CATS system respectively.

The pressure was monitored in the devolatilization system with a capacitance manometer. The real time sampling rate of this device is limited to 125 Hz. This was found adequate to track the overall light gas evolution in real time.

The light gas evolution was monitored in real time by a Nicolet FTIR in the rapid scan mode. The rapid scan feature of this device allow collection of data over the complete wavenumber range of the detector as fast as every 120 msec at

$8\text{ cm}^{-1}$  resolution. The amounts of identified gaseous species are determined by high resolution ( $0.5\text{ cm}^{-1}$ ) scanning of the cell immediately following the devolatilization process.

Transfer rates between the devolatilization cell and IR cell were determined by slightly pressurizing the devolatilization cell with gas standards and activating the solenoid valve (Fig. 2). The rate of gas transfer from the devolatilization chamber to the IR cell was determined to be fast compared to the rate of evolution at the heating rates used in this study.

High speed films (2 msec/frame) were made of the devolatilization process for some runs. In these cases the camera was focused either upon the glass walls of the grid chamber or upon a KBr disk suspended about 0.4 cm above part of the coal sample within the grid. The purpose of the film was to monitor the real time evolution of the tar species released by following the visible condensation and buildup of the tars on a transparent surface. Under low ambient pressure conditions ( $\ll 1$  torr) the tar molecular species are propelled in a line of sight path away from the devolatilizing coal and immediately condense upon striking a cool surface.

#### Procedure

325 mesh stainless steel screen (~ 7.5 cm long) is folded such that a screen sandwich (~ 1.00 cm wide) is formed. A fine chromel-alumel thermocouple (75-100  $\mu\text{m}$ ) bead is spot-welded to the underside of the bottom fold at the center of the screen. For some runs second or third beads are welded approximately 1.5 cm off of screen center, again to the underside of the bottom fold of the grid. The screens are prefired for the following reasons: (1) to obtain a constant tare weight; (2) to obtain nearly constant resistivity and emissivity; (3) to determine the exact control settings needed to produce a given blank screen heating rate, final temperature, and time at a final temperature.

After the prefiring, the screen is loaded with 10-25 mg of -100+325 mesh coal. The coal is vacuum dried at 105 C overnight. The sample is placed in approximately 2 cm length of the strip using the center thermocouple as the marker for the sample center. In the case of the two thermocouple runs the outer thermocouple resides about 0.5 cm from the bulk of the sample area. The "loaded" screen is repositioned in the reactor. The reactor is evacuated and the devolatilization experiment is performed.

The manner of applying power to the grid as well as the temperature monitoring differ significantly from other recent studies using heated grid techniques for rapid heating (3,4,5). For example, although other studies report spot welding a thermocouple to the grid, the weld is such that the bead is apparently positioned between the folds of the grid (5). Upon power application, the thermocouple is forced to follow programmed temperature trajectory by a monitoring-feedback system. In addition, little work has been reported for vacuum conditions despite the fact that it is well established that devolatilization under ambient pressure results in numerous secondary reactions for tar species formed in the primary, thermal devolatilization of the coal (1,6,7).

## RESULTS AND OBSERVATIONS

### Sample-Induced Temperature Deviations

Figure 5 displays a series of center thermocouple temperature profiles obtained with samples of an Appalachian province, high volatile bituminous coal using the VATS control circuit. In comparing the profiles to corresponding blank screen reference runs (Fig. 3) the deviations in the temperature-time path of the thermocouple are obvious.

Figure 6 displays a series of center thermocouple temperature profiles obtained with samples of a Rocky Mt. province, high volatile bituminous coal using the CATS control circuit. Again the sample-induced temperature deviations become obvious when comparing the profiles to the corresponding blank screen references (Fig. 4).

### The Local Nature of the Temperature Deviations

Figure 7 displays temperature profiles for center and edge thermocouples in blank and sample loaded screens, respectively. The curves indicate that the "thermal loading" of the screen by the sample is a local effect. Runs performed with no sample over the center thermocouple but with 5-10 mg of sample placed around the edge thermocouple positions gave similar results but for opposite thermocouples, i.e., the center thermocouple with no sample load reproduced the blank screen temperature-time plot while the edge thermocouple produced a plot similar to the previous, loaded center thermocouple plot. The results indicate that the sample introduces a significant thermal load in the immediate area of the screen such that the local, sample-loaded screen cannot follow the programmed screen temperature.

### Physical Loading of the Local Screen

Several types of experiments were performed to ascertain the influence of the physical characteristics of the sample on the programmed temperature profile. In these tests, samples with low volatile matter contents were employed. Figure 8 displays several blank and sample loaded temperature profiles for an anthracite coal. Figure 9 shows blank, coal loaded and resultant char loaded temperature profiles for a high volatile, Appalachian province bituminous coal. The curves obtained with samples of low volatile matter content indicate that the physical properties of the sample such as heat capacity and emissivity do indeed contribute to the local thermal loading of the screen. This perturbation of the physical state of the screen is manifested by a gradual deviation from the programmed heating rate and lower final temperatures achieved. In no case did tests with low volatile matter content produce temperature profiles such as those shown in Fig. 5 and 6. The temperature-time paths observed with coals of appreciable volatile matter are different in character than these observed with nonvolatile samples. The drop in edge thermocouple temperature (Fig. 7) indicates the screen is attempting to reach thermal equilibrium by thermal conduction under pseudo-steady state conditions.

#### Devolatilization-Induced Temperature Deviations

While Fig. 5 shows variations with programmed final temperature for a particular coal, Fig. 10 shows center thermocouple temperature plots for coals of varying rank using the VATS system. The high volatile bituminous coals appear to have a greater loading effect than coals of lower or higher rank. As noted above, the dip in the thermocouple temperature occurs as the VATS system switches the power output of the supply from the high output (temperature ramping state) to the lower output, temperature hold state. The temperature at the time of the switching is lower and the resultant dip is greater for the high volatile bituminous coals. Similar behavior occurs for lower final temperature runs with the VATS system (see Fig. 5). In these cases however the "warp" in the temperature path is not as severe. As noted above, such thermocouple behavior is not observed for non-volatile samples.

Figure 11 shows center thermocouple plots for 900 C final temperatures runs for coals of varying rank using the CATS system. Due to constant current programming in the CATS system, the instantaneous thermal power generation is different from the VATS system during the main phase of devolatilization process. Consequently, the characters of the temperature plots are different than the corresponding VATS plots for the same final temperatures (See Figs. 10 and 11). The high volatile bituminous coals again display a greater loading effect on the screen than lower or higher rank coals. However, the warp in the temperature plots are not as severe as those observed in the VATS system.

Figure 6 displays temperature curves obtained with a Rocky Mt. province, high volatile bituminous coal for different final temperature runs using the CATS system. The variation in the character of the temperature profile with programmed heating characteristics is apparent. It is to be noted that the product distribution varied significantly with heating conditions although total yield does not, as previously reported (1,2,6,7).

It is apparent from the character of the curves presented that the devolatilization process has a significant effect on the temperature history of the local screen complex. The actual temperature-time path followed is highly dependent on the devolatilization characteristics of the coal sample as well as the programmed, resistive heating of the screen. That is the observed thermocouple temperature path is the resultant of the coupled resistive heating and devolatilization process.

#### Tar and Light Gas Release Relative to the Thermocouple Temperature History

Figures 6 and 12 indicate the tar and light hydrocarbon (aliphatics) release relative to the thermocouple temperature history. In Fig. 12 the tar yields obtained for various power-on times were obtained by six independent runs for the times shown. The data indicate that the temperature and species evolution profiles are reproducible and that the temperature deviations are induced by the devolatilization process.

The data for the high volatile bituminous coals shown in Figs. 6 and 12 indicate that the tar and light hydrocarbon gases do not evolve simultaneously as has been previously assumed (8). The onset of the tar release precedes the

hydrocarbon light gas evolution for high volatile bituminous coals. For example, the data of Fig. 12 show that at 1.5 sec into a run nearly 50% of the potential tar yield has evolved while only 14% of the total CH<sub>4</sub> yield has evolved. Since the tar yield represents ~ 39% (dry basis) of the parent coal, the devolatilization process is nearly 40% complete before significant CH<sub>4</sub> evolution occurs.

To verify in real time the relative release times, high speed films of the tar release process were made in the manner described above. Several Appalachian and Rocky Mt. province high volatile bituminous coals were examined. Frame-by-frame inspection of these films were compared to the rapid scan infrared data and real time pressure and temperature data. For the coals tested:

1. The tar release was more closely associated with the initial temperature deviations.
2. The onset of the tar release precedes the onset of the light hydrocarbon release.
3. The light hydrocarbon gas evolution occurs mainly in the secondary temperature rise.
4. Rocky Mt. province high volatile bituminous coals displayed more overlap in the tar and light gas evolution than the Appalachian province high volatile bituminous coals.

#### Discussion and Summary

The results clearly demonstrate that the devolatilization process has a considerable influence on the time-temperature history of the local screen in immediate contact with the sample. Physical properties of the sample load (e.g. heat capacity, emissivity) cannot account for the character or magnitude of the non-steady state temperature deviations that are observed with volatile samples. With respect to the coal particles, the direct implication is that the temperature path is the resultant of several components: the resistive heating of the grid, the physical properties of the samples, the devolatilization properties of the sample. Once the range of devolatilization temperatures of a particular coal is achieved, the primary devolatilization process appears to dominate the temperature-time trajectory. Because the heat requirement of the primary devolatilization affects the temperature trajectory of the coal particle, a real time model of primary coal devolatilization must necessarily include a consideration of this requirement. In addition, the data appears to indicate that the heat requirement varies with the rank characteristics of the coal.

For a transient process such as rapid coal devolatilization the absolute magnitude of the heat required to vaporize the volatile components need not be large to result in a significant deviation from a programmed heating rate or a calculated heating rate of a nonvolatile particle. A modest heat requirement coupled to a sufficiently fast primary devolatilization process can cause appreciable changes in the temperature trajectory of a particle (9,10).

The results indicate that the tar release is closely coupled in time to the devolatilization-induced temperature deviations during primary devolatilization.

The onset of the tar release significantly precedes the slower light hydrocarbon gas evolution. Thus the rapid devolatilization heat requirement appears to be associated with the energy required to overcome intermolecular attractive forces (van der Waal, hydrogen bonds, dipole-dipole interactions) that exist among the mix of molecular species present in the coal. Once the devolatilization heat requirement is met, rapidly supplying additional thermal energy can result in thermal cracking of the primary tars, decreasing the tar yield while increasing light gas yields (See Fig. 6 and Ref. 1,2).

A quantitative real time model of coal devolatilization requires a quantitative estimate of the primary devolatilization heat requirement as well as real time data on the primary tar release rates and their susceptibility to thermal cracking. Provisions are being made to monitor the real time power delivered to the grid as well as the real time evolution of primary tars.

#### ACKNOWLEDGMENTS

The authors gratefully acknowledge the able technical assistance of Dave Santos and Gerald Wagner.

#### REFERENCES

1. Freihaut, J. D. and Seery, D. J., An Investigation of Yields and Characteristics of Tars Released During the Thermal Decomposition of Coal, ACS Fuel Chem. Preprints, 26, No. 1, 133 (1981).
2. Freihaut, J. D. and Seery, D. J., Evolution of Fuel Nitrogen During the Vacuum Thermal Devolatilization of Coal, ACS Fuel Chem. Preprints, 26, No. 3, 18 (1981).
3. Franklin, H. D., Mineral Matter Effects in Coal Pyrolysis and Hydropyrolysis. Thesis, MIT (1980).
4. Stangely, P. C. and Sears, P.L., Rapid Pyrolysis and Hydropyrolysis of Canadian Coals. Fuel, 60, 131 (1980).
5. Hamilton, L. H., Ayling, A. Bruce, and Shibaska, M., A New Experimental Device for Pyrolysing Coal Under Controlled Conditions Over a Wide Range of Heating Rates. Fuel, 58, 873 (1979).
6. Anthony, D. B., Howard, J. B., Hottel, H. C. and Meismner, H. P., Rapid Devolatilization of Pulverized Coal. 15th Symp. (Int.) Combustion, Combustion Institute, Pittsburgh, p. 1303 (1975).
7. Suuberg, E. M., Rapid Pyrolysis and Hydropyrolysis of Coal. Sc. D. Thesis, MIT, 1977.
8. Solomon, P. R. and Colket, M. B., Coal Devolatilization. 17th Symp. (Int.) Combustion, Combustion Institute Pittsburgh, p. 131 (1979).
9. Freihaut, J. D. and Vastola, F. J., A Computational Examination of the Effect of Coupled Heat Transport and Chemical Kinetics Upon Single Particle Coal Pyrolysis. Presented at Eastern States Combustion Institute Mtg., Miami, Fla. (1978).
10. Freihaut, J. D., A Numerical and Experimental Investigation of Rapid Coal Pyrolysis. Thesis, Penn State Univ. (1980).

## EXPERIMENTAL NETWORK

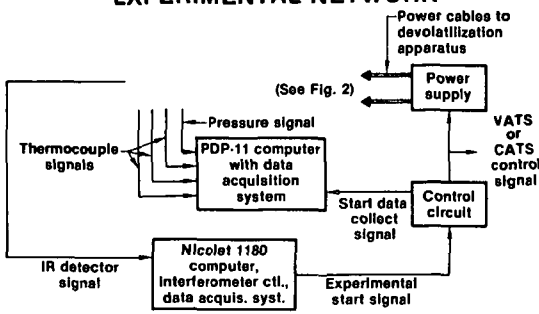


Fig. 1

## HEATED-GRID DEVOLATILIZATION APPARATUS

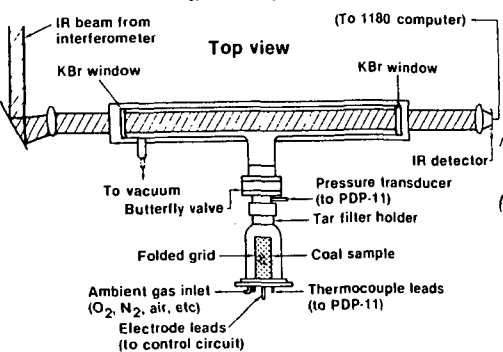


Fig. 2

## BLANK SCREEN TEMPERATURE — TIME

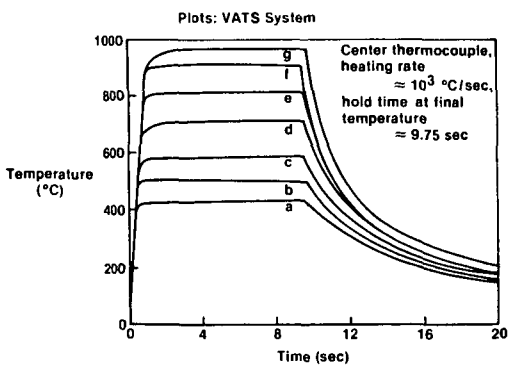


Fig. 3

## TEMPERATURE — TIME PLOTS CATS System

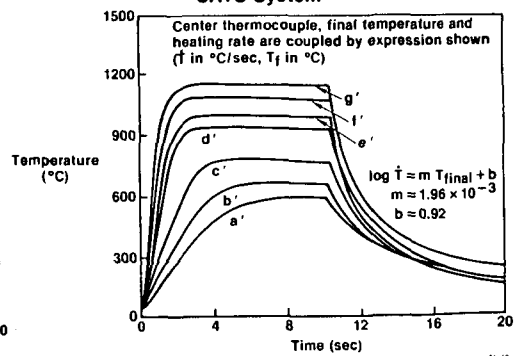


Fig. 4

### CENTER THERMOCOUPLE TEMPERATURE — TIME

Histories for devolatilization with hv bit. Appal. coal

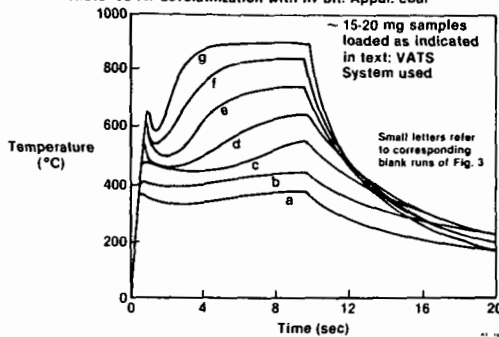


Fig. 5

### CENTER THERMOCOUPLE TEMPERATURE — TIME

Histories for devolatilization with hv bit. Rocky Mt. coal

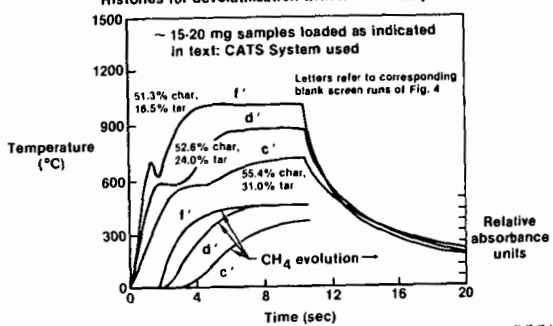


Fig. 6

### CENTER AND EDGE THERMOCOUPLE TEMPERATURE HISTORIES

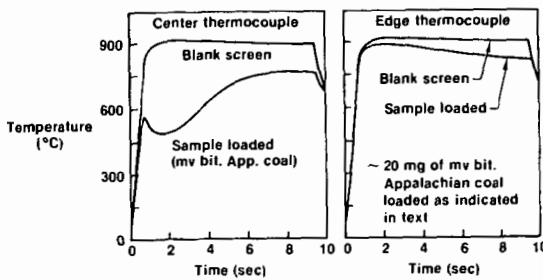


Fig. 7

### BLANK AND SAMPLE-LOADED THERMOCOUPLE PLOTS: ANTHRACITE

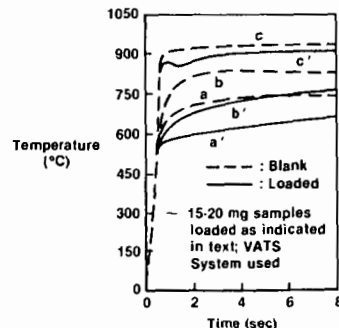


Fig. 8

### COAL vs CHAR LOADING OF SCREEN

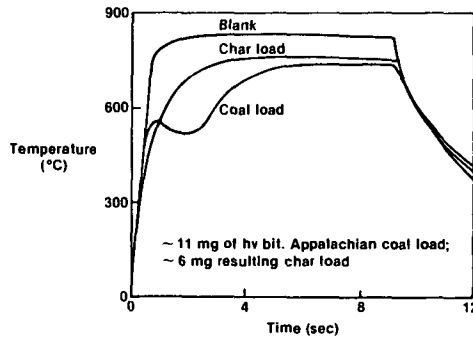


Fig. 9

### VARIATION OF THERMAL LOADING WITH RANK-VATS SYSTEM

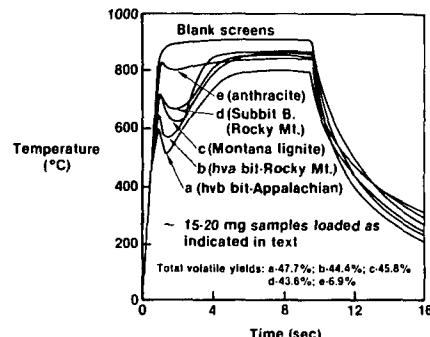


Fig. 10

### VARIATION OF THERMAL LOADING WITH RANK — CATS SYSTEM

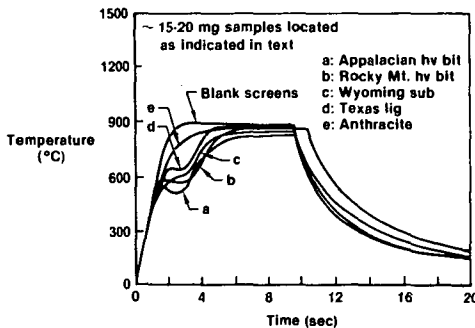
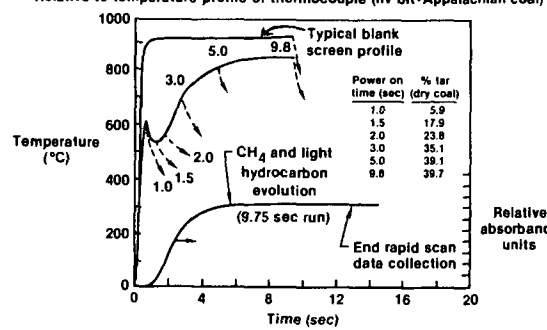


Fig. 11

### TAR AND LIGHT HYDROCARBON YIELDS

Relative to temperature profile of thermocouple (hv bit-Appalachian coal)



— Power-on; - - - Cooling curves (power off); numbers at various points represent total time of power on during run. 9.8 sec run: 54.1% tar; 39.7% gas

Fig. 12